Pore Water Velocity and Residence Time Effects on the Degradation of 2,4-D during Transport

HEIKO W. LANGNER,
WILLIAM P. INSKEEP,*
HESHAM M. GABER,[†] WARREN L. JONES,[‡]
BHABANI S. DAS, AND JON M. WRAITH

Department of Plant, Soil, and Environmental Sciences, Montana State University, Bozeman, Montana 59717

Model predictions of fate and transport of organic solutes in soils and groundwater are sensitive to assumptions concerning rates of microbial degradation. We studied the independent effects of residence time (RT) and pore water velocity (v) on the degradation of 2,4-dichlorophenoxyacetic acid (2,4-D) by employing a series of unsaturated soil column experiments (continuous pulse concentration = 1 mg L^{-1}) with varying column lengths and v. While 2,4-D degradation under batch conditions was best described by a logistic rate expression, analysis of the 2,4-D breakthrough curves (BTCs) showed that (i) observed 2,4-D degradation rates were consistent with a first-order kinetic model and (ii) a single set of independently determined rate parameters from batch experiments could not describe 2,4-D degradation for all transport conditions. Apparent first-order degradation rate constants obtained from column data were found to be independent of column RT, but increased with decreasing v, especially at $v < 1$ cm h^{-1}. Variations in apparent degradation rate constants with changing v may be due to effects of v on microbial attachment and distribution, local opportunity times required for maximum 2,4-D degradation, or nutrient desorption rates from the soil solid phase. Results from this study emphasize the difficulty in obtaining accurate model predictions using a single set of degradation rate parameters for all transport conditions, and the need to develop a better understanding of coupled processes involving contaminant degradation and transport.

Introduction

Accurate model predictions of the fate of organic solutes in soils require appropriate rate equations describing microbial degradation and appropriate estimates of degradation rate parameters (e.g., rate constants). Uncertainties in rate expressions and/or rate parameters can result in significant variation in model predictions of solute fate and transport. For example, for weakly sorbing pesticides such as 2,4-D, an increase in the half-life from 10 to 20 d could result in an increase in the fraction of solute leached by approximately 2 orders of magnitude (*1*). Similarly, model simulations showed that a 15–22% variation in the first-order degradation

* Corresponding author e-mail: usswi@montana.edu; telephone: 406-994-5077; fax: 406-994-3933.
† Present address: Department of Soil and Water Sciences, College of Agriculture, University of Alexandria, El-Shatby, Alexandria, Egypt.
‡ Department of Civil Engineering, Montana State University.

rate constant led to a 100% uncertainty in the amount of aldicarb leached below the root zone (*2*).

The majority of fate and transport models use a first-order kinetic expression to describe microbial degradation during transport (*3–6*), due primarily to the simplicity and convenience of assuming that the rate constant (and half-life) is independent of substrate concentration. Certainly there are examples in the literature that demonstrate situations where first-order kinetic expressions have been suitable (*7, 8*) and unsuitable (*8–10*) for describing solute fate and transport. Estrella et al. (*8*) used first-order kinetics to describe steady-state 2,4-D effluent concentrations (eluent [2,4-D] = 100 mg L^{-1}) under saturated transport conditions; however, under unsaturated conditions, effluent concentrations of 2,4-D increased to a maximum value and then decreased to zero. Similar shapes of solute breakthrough curves (BTCs) were reported by Kelsey and Alexander (*9*) using *p*-nitrophenol (10 mg L^{-1}) and by Pivetz and Steenhuis (*10*) using 2,4-D (50 μg L^{-1}). Under these circumstances, rate expressions based on microbial growth (e.g., Monod or logistic growth models) are necessary for adequate descriptions of solute transport.

Independent of the model used to describe microbial degradation during transport, there is additional uncertainty regarding the appropriate choice of rate parameters necessary for predicting degradation. Estrella et al. (*8*) showed that degradation rate parameters determined under batch conditions were not suitable for predicting 2,4-D BTCs. In addition, results obtained by Kelsey and Alexander (*9*) suggest a strong dependence of *p*-nitrophenol degradation rate parameters on the solute flow regime (path length and flow rate). If these findings are generally true for organic solutes subject to microbial degradation, then our ability to predict degradation across a wide range of transport conditions using a single set of batch-determined parameters is reduced significantly. For first-order kinetics, increases in residence time (RT) are expected to result in increases in the total amount of substrate degraded during transport. However, there is little published information concerning potential effects of pore water velocity (v) on apparent degradation rate parameters observed during transport. Since most experiments employ constant column lengths, changes in RT are generally associated with changes in v and vice-versa. Consequently, the objectives of this study were to (i) test the applicability of first-order and logistic growth models for describing 2,4-D degradation, at concentrations representative of typical field application rates, across a wide range in column conditions; (ii) determine the applicability of degradation rate parameters derived under batch conditions for describing 2,4-D degradation across a wide range in column conditions; and (iii) separate effects of column RT and v on degradation rate parameters determined from transport experiments.

Materials and Methods

Soil. All experiments were performed using Flathead fine sandy loam (coarse-loamy, mixed Pachic Udic Haploboroll) surface soil (0–0.20 m) collected at the Northwest Agricultural Research Center (Creston, MT). After collection, the soil was air-dried, sieved (<2 mm), and stored at room temperature prior to the experiments. This soil contained 2.0% organic C, 3% clay, 12% silt, and 85% sand and had a soil pH of 7.0 (1:1 soil:water mass ratio). Equilibrium sorption experiments resulted in a linear adsorption isotherm of 2,4-D to this soil [$Q = K_d C$, where Q is the sorbed phase 2,4-D concentration

TABLE 1. Experimental Conditions for the Column Experiments

column length (L) (cm)	column residence time (RT)[a] (h)	pore water velocity (ν)[b] (cm h⁻¹)	soil water content (θ) (m³ m⁻³)	bulk density (ρ) (Mg m⁻³)	dispersion coefficient (D)[c] (cm² h⁻¹)	experimental ID
			Nonsterile Columns			
9.5	4.9	1.9	0.27	1.32	1.53	RT5L9
	20.4	0.5	0.30	1.27	1.35	RT16L9
	52.8	0.2	0.26	1.32	0.22	RT48L9
28.5	5.5	5.2	0.35	1.30	4.97	RT5L28
	18.7	1.5	0.30	1.44	1.07	RT16L28
	50.0	0.6	0.26	1.54	0.48	RT48L28
85.5	15.0	5.7	0.37	1.34	1.12	RT16L85
	51.5	1.7	0.35	1.35	1.20	RT48L85
			Sterile Column			
8.2	13.4	0.6	0.34	1.49	0.22	RT16L9S

[a] $RT = L/\nu$. [b] $\nu = J_w/\theta$, where J_w is volumetric water flux density (Darcy velocity). [c] Determined from fitting ^3H_2O BTCs.

(mg kg⁻¹), K_d is the linear batch sorption coefficient (L kg⁻¹), C is the aqueous phase 2,4-D concentration (mg L⁻¹)] when C was less than 1 mg L⁻¹ ($K_d = 0.66 \pm 0.02$ L kg⁻¹, $r^2 = 0.92$).

Batch Degradation Experiments. Batch degradation studies were conducted using 10-g samples of soil in gastight Erlenmeyer flasks containing two ports for continuous gas exchange. Soil water contents (θ) were varied (0.25, 0.32, and 0.38 m³ m⁻³, in triplicate) to evaluate the effect of variable θ on 2,4-D degradation using an initial aqueous phase 2,4-D concentration of 1.0 mg L⁻¹. Preliminary studies showed that initial degradation rates were sensitive to the duration of prewetting the soil prior to 2,4-D application. Therefore, additional experiments were conducted using prewetted soil ($\theta = 0.21$ m³ m⁻³ for 3 d prior to initiation of degradation experiments) in an attempt to simulate the conditions of the transport experiments discussed below. Additional degradation experiments were conducted with slurries (shaken on a rotary shaker at 130 rpm) to reduce potential effects of rate-limited transport of 2,4-D to sites of microbial degradation. These experiments were conducted using a soil (prewetted):water ratio of 1:3 (g:g) and two initial 2,4-D concentrations (1.0 and 0.1 mg L⁻¹): 1.0 mg L⁻¹ was chosen to expose the microorganisms to the same initial 2,4-D concentration as in the nonstirred experiments, and 0.1 mg L⁻¹ represented a similar absolute mass of 2,4-D per gram of soil as used in the nonstirred experiments.

The applied 2,4-D solutions contained approximately 5×10^5 Bq L⁻¹ carboxyl-¹⁴C-labeled 2,4-D (specific activity of 4.70×10^{11} Bq mol⁻¹, Sigma Chemical Co., St. Louis, MO) in addition to unlabeled 2,4-D (analytical grade 2,4-D with a stated purity of 99%, Aldrich Chemical Co., Milwaukee, WI). All liquids added to the batch reactors contained a background solution of 3 mM $CaCl_2$. The headspace was continuously purged with humidified, CO_2-free air at a flow rate of approximately 100 mL h⁻¹, which was then passed through 10 mL of 0.5 M NaOH to trap $^{14}CO_2$. Rates of $^{14}CO_2$ evolution were determined by periodically analyzing for ¹⁴C in the NaOH traps (Packard 2200CA liquid scintillation analyzer, Packard Instrument Co., Downers Grove, IL).

Column Transport Experiments. A series of soil column experiments with varying column lengths and solute flow rates was performed to separate effects of ν and RT on the rate of 2,4-D degradation during transport (Table 1). Soil columns were prepared by uniformly packing air-dried soil into PVC tubes with an inner diameter of 5.1 cm. Bulk densities (ρ) were 1.4 Mg m⁻³ (± 0.1 Mg m⁻³) and column lengths (L) were 9.5, 28.5, or 85.5 cm leaving a headspace of 1 cm. The ends of the columns were secured with polycarbonate caps containing rubber O-rings. The bottom end caps supported porous plastic plates with an air entry pressure of 100 kPa (Soil Measurement Systems, Tucson, AZ). Columns were equipped with an air entry port near the

bottom and an air outlet in the top end cap. Eluent was supplied with a precision syringe pump (Soil Measurement Systems) at variable rates depending on the desired ν. Fraction collectors (Retriever II, ISCO Inc., Lincoln, NE) housed in vacuum chambers (Soil Measurement Systems) were used to collect effluent (up to 13 mL per sample) while maintaining a constant negative pressure at the bottom plates of the soil columns (12). Peristaltic pumps were used to provide a continuous airstream of approximately 15−40 mL h⁻¹ to the air inlet ports (the higher flow rates were used in the longer soil columns), as a mechanism to minimize anaerobic conditions within the columns.

Soil columns were wetted from the bottom over 8−48 h depending on the column length, after which the bottom plate pressure was set to −30 kPa and 3 mM $CaCl_2$ was supplied to the top of the column. Soil water content (θ) was monitored daily by detaching and weighing the columns throughout individual experiments. The desired column residence times (RT = L/ν) were achieved by varying the eluent delivery rate. Target residence times were 5.3, 16, and 48 h; however, deviations in eluent pump rates and θ resulted in actual RT values within 27% of the targeted values (Table 1). Although all calculations and conclusions were based on actual values of RT and ν, the target RT values are used in the text for simplicity.

After steady-state flow conditions were established (constant θ and ν), the eluent solution was switched from 3 mM $CaCl_2$ to a continuous pulse of 1.0 mg L⁻¹ 2,4-D containing ¹⁴C-carboxyl-labeled 2,4-D (specific activity of 1.2×10^5 to 5.7×10^5 Bq L⁻¹ depending on the anticipated amount of degradation), ^3H_2O as a tracer (specific activity approximately 7×10^4 Bq L⁻¹), and 3 mM $CaCl_2$. Column effluent fractions were analyzed for ¹⁴C and ³H using liquid scintillation. The evolution of $^{14}CO_2$(g) was periodically determined by sampling CO_2 traps located at the air outlet port and within the vacuum chamber. Selected effluent samples were analyzed before and after acidification and purging with N_2(g) to determine the contribution of carbonate-¹⁴C to total ¹⁴C in the effluent. Effluent samples from representative experiments were also analyzed using HPLC radioisotope detection to determine the fraction of total ¹⁴C present as 2,4-D.

Experiments were continued until approximate steady-state concentrations of 2,4-D were obtained in the effluent (9−14 pore volumes), at which time the eluent was switched back to 3 mM $CaCl_2$. Column experiments were terminated when the effluent ¹⁴C concentrations approached zero. Soil columns were frozen until they were sectioned into 3.5 cm (upper 9.5 cm) or 9.5 cm (below 9.5 cm) segments. The individual segments were analyzed for soil residual ¹⁴C using biological oxidation (R. J. Harvey Instrument Corp., Hillsdale, NJ) and liquid scintillation.

A sterile column experiment ($L = 8.2$ cm, RT = 13.4 h) was performed to separate biotic and abiotic factors influencing transport of 2,4-D. We premixed 250 g of soil [preincubated for 2 d at a water content of 0.2 L (kg of soil)$^{-1}$] with crystalline $HgCl_2$ at a rate of 1.0 g (kg of soil)$^{-1}$ (13). All column parts, tubing, and background solutions were either autoclaved twice or stored in 70% ethanol for several days before assembling the column. The soil was packed uniformly into the column and treated as the other columns.

Modeling Approaches

Degradation Under Batch Conditions. (A) Logistic Growth Model. A solution to a logistic growth model was used to describe the degradation kinetics of 2,4-D in the batch degradation experiments. The logistic model is based on the Monod equation relating bacterial growth rate and concentration of a single substrate (14–16). Monod kinetics can be expressed as

$$\mu = \frac{\mu_{max}C}{K_s + C} \qquad (1)$$

where $\mu = dX/dt(1/X)$ is the specific growth rate (h^{-1}), μ_{max} is the maximum specific growth rate (h^{-1}), C is the aqueous-phase 2,4-D concentration (mg L^{-1}), K_s is the half-saturation constant for growth (mg L^{-1}), and X is the 2,4-D concentration required to produce the degrader population density present at time t (mg L^{-1}). This expression is based on the assumption that only aqueous-phase 2,4-D can be degraded by both attached and suspended bacteria, which has been shown to be appropriate for 2,4-D degradation in soils (17). When $K_s \gg C$, the Monod equation reduces to the logistic rate expression:

$$\frac{dX}{dt} = k_L CX \qquad (2)$$

where $k_L = \mu_{max}/K_s$ is the logistic rate constant (L mg^{-1} h^{-1}). It is commonly assumed that a constant fraction of carbon from degrading 2,4-D is incorporated into biomass and the remaining evolves as CO_2 (15). On the basis of this assumption, the following mass-balance relationship applies:

$$S - S_0 = -\frac{X - X_0}{Y} = -\frac{P - P_0}{1 - Y} \qquad (3)$$

where S represents the total (sorbed plus aqueous phase) 2,4-D concentration (mg L^{-1}), Y is the yield or fraction of 2,4-D converted into biomass during 2,4-D degradation, P is the cumulative amount of 2,4-D converted into CO_2 (mg L^{-1}), and the subscript 0 designates the initial parameter values. Assuming a linear sorption isotherm, the total substrate concentration may be expressed as $S = C + (\rho/\theta)K_dC$, where ρ is bulk density (Mg m^{-3}). This expression can be substituted into eq 3 and rearranged to yield

$$C = \frac{S_0 - (X - X_0)/Y}{1 + (\rho/\theta)K_d} \qquad (4)$$

After substitution of eq 4, eq 2 may be integrated, and the result can be written in terms of P using eq 3:

$$P = \frac{(z - 1)(1 - Y)X_0}{zX_0/S_0 + Y} \qquad (5)$$

where

$$z = \exp\left(\frac{S_0 + X_0/Y}{1 + (\rho/\theta)K_d}k_L t\right) \qquad (6)$$

The parameters of the logistic model (X_0, Y, and k_L) were estimated by fitting $^{14}CO_2$ evolution data from the batch degradation experiments to eq 5 using nonlinear least-squares optimization.

(B) First-Order Degradation Model. A batch-derived first-order degradation rate constant (k_{1b}) was obtained by fitting a first-order degradation expression to the $^{14}CO_2$ evolution data of the batch experiment (prewetted moist soil). If only liquid-phase 2,4-D can be degraded (17), the first-order degradation equation for substrate disappearance may be written as $dS/dt = -k_{1b}C$. Assuming the transformation of a constant fraction of degrading 2,4-D into CO_2 (as followed by carboxyl-^{14}C), the mass-balance relationship in eq 3 applies. As shown with the logistic model, C in the first-order degradation equation can be substituted using eq 4, and the resulting equation can be integrated to yield (after substitution of eq 3):

$$P = (1 - Y)\left[1 - \exp\left(-\frac{k_{1b}}{1 + (\rho/\theta)K_d}t\right)\right]S_0 \qquad (7)$$

Least-squares optimization was used to estimate k_{1b} and Y for CO_2 evolution data of the batch experiment with prewetted, moist soil.

Transport Experiments. (A) Fitted Parameters. Tritiated water (^3H_2O) breakthrough curves (BTCs) were used to obtain apparent dispersion coefficients (D) for each column and to test for the presence of physical nonequilibrium (18–20). BTCs curves for ^3H_2O were fit to both the local equilibrium (LE) and two-region physical nonequilibrium (physical NE) versions of the advection−dispersion equation (ADE) using a nonlinear least-squares parameter optimization method (CXTFIT2; ref 6). Retardation factors (R_f) were derived from the linear 2,4-D batch sorption coefficient (K_d), column water contents (θ), and bulk densities (ρ) as $R_f = 1 + (\rho/\theta)K_d$. Values of D and R_f were used to predict BTCs for 2,4-D in the sterile column experiments, for comparison to observed data. A solution to the ADE with a two-site chemical nonequilibrium (chemical NE) option (6) was also fit to the 2,4-D BTC of the sterile column and the nonequilibrium parameters ω and β (ref 21; $\beta = [1 + (\rho/\theta)FK_d]/R_f$, where F is the fraction of sorbent for which sorption is instantaneous; $\omega = [k_2(1 - \beta)R_fL]/v$, where k_2 is the desorption rate constant) were obtained in order to evaluate potential contributions of chemical non-equilibrium.

(B) Model Predictions. 2,4-D BTCs of all nonsterile columns were predicted independently using dispersion coefficients (D) from ^3H_2O BTCs, R_f values from 2,4-D sorption isotherms, and two different approaches for describing microbial degradation (logistic growth and first-order models). The logistic degradation model (eq 2) was combined with the LE-based ADE to yield:

$$R_f\frac{\partial C}{\partial t} = D\frac{\partial^2 C}{\partial x^2} - v\frac{\partial C}{\partial x} - \frac{k_L CX}{Y} \qquad (8)$$

where C is the volume averaged 2,4-D concentration in the aqueous phase (mg L^{-1}), x is soil depth (cm), and the other symbols are as defined earlier. Equations 8 and 2 were numerically solved for the initial conditions $C(x,0) = 0$ and $X(x,0) = X_0$, and the boundary conditions $C(0, t) = C_0$ and $\partial C/\partial x = 0$ at $x = \infty$ (22) using a fully implicit finite difference scheme. All logistic model parameters were obtained independently from batch degradation experiments.

Likewise, a first-order rate constant (k_{1b}) from batch experiments (prewetted soil) was used to independently predict (CXTFIT2, ref 6) 2,4-D BTCs for all nonsterile columns. In addition, an analytical solution to the ADE containing a first-order decay term (23) was used to estimate steady-state
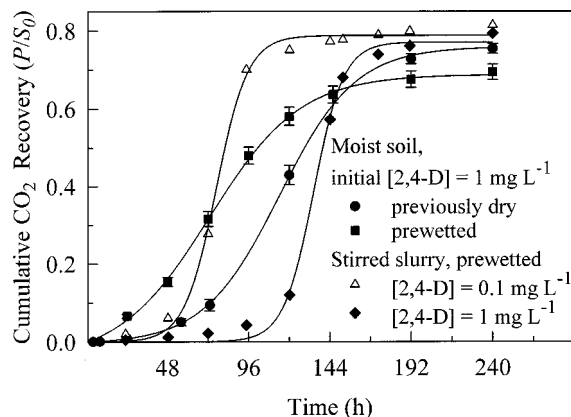
FIGURE 1. Degradation of [^{14}C]2,4-D (measured as fraction of total added ^{14}C recovered as ^{14}CO$_2$, P/S_0) in batch experiments performed under various conditions. Error bars for moist, previously dry soil were generated using data from all soil water contents tested. Filled symbols represent initial aqueous phase 2,4-D concentrations of 1.0 mg L^{-1}; open symbols represent 0.1 mg L^{-1} initial aqueous phase 2,4-D concentration.

first-order degradation rate constants k_{1s} (h^{-1}) from the 2,4-D BTCs. The solution in van Genuchten and Alves (case C1, ref *23*) was solved for k_{1s} to obtain (assuming relative concentrations):

$$k_{1s} = \frac{\ln C_s(D \ln C_s - x\nu)}{x^2} \qquad (9)$$

where C_s is the relative steady-state effluent concentration of 2,4-D (i.e., weighted average of C/C_0 at steady state) and the other symbols are as defined earlier. Values of k_{1s} were calculated for each column based on known values of D, ν, and x (Table 1).

Results

2,4-D Degradation under Batch Conditions. Degradation curves of 2,4-D under batch conditions show the effects of soil wetness, pretreatment, mixing environment, and initial substrate concentration (Figure 1). The absence of ^{14}CO$_2$ evolution in autoclaved soils supported the assumption that abiotic sources of 2,4-D degradation were insignificant under batch conditions. The sigmoidal shape of the degradation curves as well as the low initial aqueous-phase 2,4-D concentrations justify the use of a logistic degradation model to describe the batch degradation data (ref *24*; Table 2). Variations in θ did not significantly affect rates of ^{14}CO$_2$ evolution within the range tested; hence, the data presented in Figure 1 for previously dry, moist soil are averages from all batch reactors at $\theta = 0.25$, 0.32, and 0.38 m^3 m^{-3}. Water contents of all column transport experiments (0.26–0.37 m^3 m^{-3}) were bracketed by this range; consequently, variations in θ within column experiments are not expected to cause significant variations in 2,4-D degradation rate. However, soils prewetted for 3 d prior to 2,4-D application exhibited more rapid onset of 2,4-D degradation as compared to soil not prewetted (resulting in a 10-fold increase in model estimates of X_0, Table 2). The estimated parameters obtained with prewetted, moist soil were used in the logistic transport model to predict 2,4-D BTCs under column conditions, because the conditions most closely approximated column pretreatment and water content conditions.

Changing from a stationary, moist soil environment to a well-stirred soil slurry generally resulted in lower estimates of X_0 (e.g., $X_0 = 0.02$ mg L^{-1} for the prewetted, moist soil versus $X_0 = 6 \times 10^{-8}$ mg L^{-1} for the prewetted soil slurry). A 10-fold decrease in initial 2,4-D concentration (to 0.1 mg

L^{-1}) in the slurry experiments resulted in a shorter period of lower degradation rate preceding the rapid linear rate, a 10-fold increase in k_L, and a 100-fold increase in X_0 as estimated by the curve-fitting procedure (Table 2). A similar dependence of 2,4-D degradation kinetics on initial 2,4-D concentration was reported by Parker and Doxtaeder (*25*).

Behavior of ^{3}H$_2$O during Transport Experiments. Tritiated water (^{3}H$_2$O) BTCs were analyzed to obtain column dispersion coefficients (D) and to test for the presence of physical nonequilibrium (NE) conditions (CXTFIT2; refs *6* and *18–20*). This analysis suggested that physical NE processes were not significant in any of the columns (*26, 27*).

Sterile Control Column Experiment. The lack of detectable ^{14}CO$_2$ evolution in the gas phase of the sterile column suggested that abiotic pathways of 2,4-D degradation were insignificant under these conditions. Also, 98% of the applied [^{14}C]2,4-D was recovered in the column effluent, indicating that only a small fraction of the applied 2,4-D was sorbed irreversibly to the soil. This provides important evidence that residual soil ^{14}C measured in nonsterile columns was present as biomass ^{14}C (or as degradation products with different sorption characteristics than 2,4-D) rather than as irreversibly bound 2,4-D.

To investigate the contribution of NE sorption processes under abiotic conditions, the observed 2,4-D BTC from the sterile column was compared to predicted and fitted BTCs using transport models based on the LE and two-site chemical NE assumptions (ref *6*; Figure 2). The BTC was reasonably well described by a prediction based on the LE model, using D (0.22 cm^2 h^{-1}, Table 1) from the ^{3}H$_2$O BTC and a batch-derived retardation factor $R_f = 3.89$ (Figure 2); however, some deviations from the observed BTC are evident in both the breakthrough and elution fronts. These deviations may be explained by inadequacy of batch K_d (R_f) values or as true chemical NE. For example, fitting the LE model by optimizing R_f improved the description of the observed BTC by shifting the positions of the breakthrough and elution fronts (Figure 2). Alternatively, the chemical NE model with fixed R_f (3.89) and optimized nonequilibrium parameters ($\beta = 0.76$, $\omega = 0.42$) provided an excellent fit to the observed BTC ($r^2 = 0.995$) with a good description of early breakthrough and tailing. The improved description using the chemical NE model and given that the ^{3}H$_2$O BTC showed no physical NE suggest contributions of chemical nonequilibrium to 2,4-D transport under conditions specific to the sterile column control (i.e., $\nu = 0.6$ cm h^{-1}, RT = 13.4 h).

It should be emphasized that although chemical NE causes shifts in the breakthrough and elution fronts of the BTCs, it does not affect the final position of the steady-state effluent concentration, provided that the 2,4-D pulse is long enough to achieve steady-state 2,4-D concentrations. In fact, it can be shown that, at steady state, eq 9 is valid for chemical or physical NE models as well as the LE model (*7*). As will be discussed further, potential contributions of chemical NE in nonsterile columns may have varied with column conditions (e.g., ν) but did not have a significant impact on the identification of steady-state 2,4-D effluent concentrations.

2,4-D Transport under Nonsterile Conditions. Acidification of effluent samples with HCl and subsequent purging with N$_2$ did not reduce the concentrations of ^{14}C, indicating that carbonate-^{14}C concentrations in the column effluents were insignificant. Analysis of selected effluent samples using HPLC radioisotope detection showed that the majority of ^{14}C was in fact [^{14}C]2,4-D. This observation coupled with the nearly complete 2,4-D recovery in the effluent of the sterile control column led us to the simplifying assumptions that (i) ^{14}C found in the column effluent was representative of [^{14}C]2,4-D and (ii) ^{14}CO$_2$ in the gas phase as well as residual ^{14}C in the soil represented microbiologically altered or degraded compound.

TABLE 2. Estimated Parameters Obtained by Fitting the Logistic Growth Model to CO_2 Evolution Data of 2,4-D Degradation Experiments Conducted under Various Batch Conditions

experimental conditions			fitting parameters			
soil pretreatment	θ^a (m³ m⁻³)	S_0 (mg L⁻¹)	X_0 (mg L⁻¹)	Y	k_L (L mg⁻¹ h⁻¹)	r^2
previously dry	0.25	1.0	0.0022 (0.0004)[b]	0.26 (0.005)	0.20 (0.008)	1.00
	0.32	1.0	0.0016 (0.0003)	0.24 (0.004)	0.17 (0.006)	0.999
	0.38	1.0	0.0010 (0.0001)	0.23 (0.003)	0.16 (0.004)	0.999
prewetted	0.35	1.0	0.020 (0.003)	0.31 (0.008)	0.13 (0.008)	0.992
	4.2 (slurry)	1.0	6×10^{-8} (7×10^{-8})	0.23 (0.01)	0.14 (0.01)	0.998
		0.1	6×10^{-6} (4×10^{-6})	0.21 (0.009)	1.30 (0.13)	0.997

[a] Calculated from gravimetric water content assuming $\rho = 1.4$ Mg m⁻³. [b] Values in parentheses designate standard errors.
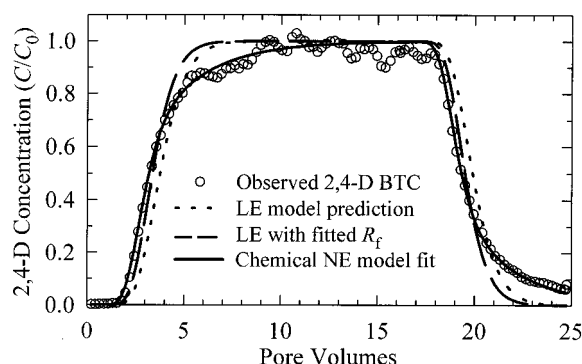

FIGURE 2. Observed and predicted [LE model using independent estimates of R_f (3.89) and D (0.22 cm² h⁻¹)] 2,4-D breakthrough curves (BTCs) for sterile column experiment. Fitted BTCs were generated using (i) the LE model where R_f was optimized (3.49) and (ii) the chemical nonequilibrium model where nonequilibrium parameters were optimized ($\beta = 0.76$, $\omega = 0.42$) using fixed R_f (3.89) and D (0.22 cm² h⁻¹).

Under nonsterile column conditions, the amount of 2,4-D degraded varied considerably as a function of column residence time (RT) and pore water velocity (v, Figure 3). Most 2,4-D BTCs exhibited steady-state 2,4-D effluent concentrations (C_s) after approximately 6 pore volumes (10 pore volumes for experiments with RT = 5.3 h, Figure 3) with values ranging from 0.063 to 0.92 across all conditions (Table 3). Amounts of 2,4-D recovered in column effluent always decreased with increasing column RT among experiments at constant column length. For example, at $L = 9.5$ cm, the fraction of applied 2,4-D recovered in column effluent dropped from 0.89 (RT = 5.3 h) to 0.58 (16 h) and 0.07 (48 h). This is consistent with the expected relationship between 2,4-D degradation and column RT (i.e., increases in time available for 2,4-D degradation result in greater amounts of 2,4-D degraded).

The effect of v on degradation can be understood qualitatively by comparing effluent 2,4-D recoveries across columns with similar RTs but varying L. At constant RT, the amounts of 2,4-D degraded always increased with decreasing v (or decreasing L, Table 3). For example, at RT = 48 h, the fractions of applied 2,4-D recovered in column effluent decreased from 0.67 ($L = 85.5$ cm, $v = 1.8$ cm h⁻¹) to 0.18 ($L = 28.5$ cm, $v = 0.6$ cm h⁻¹) and 0.07 ($L = 9.5$ cm, $v = 0.2$ cm h⁻¹). Similar results for the dependence of p-nitrophenol degradation on both the RT and v were obtained by Kelsey and Alexander (9), although effluent concentrations of p-nitrophenol always dropped to zero after 4 d.

In our study, lower effluent 2,4-D recoveries always corresponded to higher amounts of ¹⁴C recovered as ¹⁴CO₂(g) and soil residual ¹⁴C (Table 3). However, as values of ¹⁴C recovered in effluent decreased (i.e., experiments exhibiting greater 2,4-D degradation), total recoveries of applied ¹⁴C

decreased from 96% to 48%. Values of ¹⁴C in effluent samples were corroborated with direct identification of [¹⁴C]2,4-D using HPLC, and analysis of residual soil ¹⁴C using biological oxidation was both reproducible (6% mean deviation between replicate soil samples) and accurate (recoveries 94.5 ± 1.0%). Consequently, we believe that the lower total ¹⁴C recoveries in experiments that exhibited the greatest 2,4-D degradation were due to loss of ¹⁴CO₂(g) through gas leaks or loss of ¹⁴CO₂ from scintillation fluid and did not affect values of C_s used to estimate apparent first-order rate constants. To minimize the effects of gas leaks in similar batch or column systems, air flow through the system could be attained by using a vacuum at the air outlet port instead of applying pressure at the air inlet port.

Transport Simulations with Logistic Growth Model. Independent estimates of model input parameters, obtained from ³H₂O BTCs (D, Table 1), batch sorption isotherms (R_f), and the batch degradation experiment with prewetted, moist soil ($X_0 = 0.02$ mg L⁻¹, $Y = 0.31$, $k_L = 0.13$ L mg⁻¹ h⁻¹, Table 2) were used to predict 2,4-D BTCs using a numerical solution to the ADE (eq 8). Given this set of input data, the logistic model did not accurately predict the observed 2,4-D BTCs (Figure 3). All of the predicted curves show a period of slow growth (low degradation rate) followed by a period of rapid growth (high degradation rate) where the predicted effluent substrate concentration diminishes dramatically until C_s approaches zero. We also performed sensitivity analyses of the effects of logistic model parameters on 2,4-D BTCs, which documented that uncertainty of independent parameter estimates was not responsible for lack of agreement between predicted and observed 2,4-D BTCs. This disagreement is due to the general inability of the logistic model to predict steady-state solute concentrations other than 0 or 1.

Transport Modeling with First-Order Degradation. Although first-order kinetics did not adequately describe 2,4-D degradation under some batch conditions (primarily due to observed lag phases lasting 2−5 d), experiments performed at initial concentrations of 0.1 and 1 mg of 2,4-D L⁻¹ (stirred slurry, prewetted soil) showed that maximum 2,4-D degradation rates exhibited first-order dependence on initial 2,4-D concentration. Furthermore, the batch experiment using prewetted soil (most similar to column conditions) reduced the lag phase, and the degradation data (36−240 h) could be adequately described using a first-order model, where $k_{1b} = 0.066 \pm 0.003$ h⁻¹ and $Y = 0.28 \pm 0.01$ ($r^2 = 0.98$). Predicted 2,4-D BTCs using a first-order kinetic model ($k_{1b} = 0.066$ h⁻¹) coupled with the local equilibrium (LE) ADE (Figure 3) accurately reflected (i) the development of nonzero steady-state effluent 2,4-D concentrations (C_s) and (ii) the general effects of RT on values of C_s where increasing RT resulted in decreasing values of C_s. However, a single batch-determined k_{1b} value did not accurately describe 2,4-D degradation and 2,4-D BTCs for all column conditions.
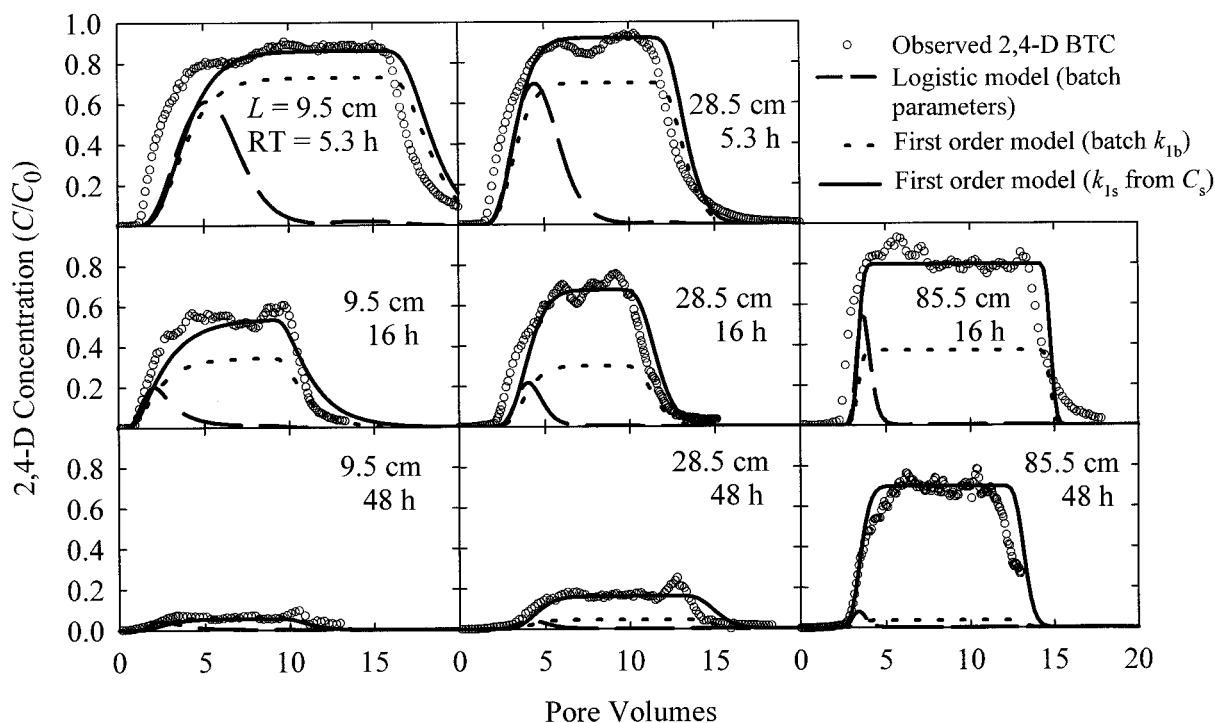
FIGURE 3. Comparison of observed and predicted 2,4-D BTCs for nonsterile column experiments. Predicted BTCs were generated using (i) the LE model with logistic degradation kinetics and independent estimates of R_f (from $K_d = 0.66$ L kg^{-1}), D (Table 3), X_0 (0.02 mg L^{-1}), Y (0.31), and k_L (0.13 L mg^{-1} h^{-1}); (ii) the LE model with first-order degradation kinetics and independent estimates of R_f, D, and k_{1b} (0.066 h^{-1}); and (iii) the LE model with first-order degradation kinetics and independent estimates of R_f, D, and k_{1s} (calculated from C_s using eq 9, Table 4).

TABLE 3. Fate of 2,4-D in Soil Column Experiments

experimental ID	$C_s{}^a$	$k_{1s}{}^b$ (h^{-1})	half-life^b (d)	^{14}C recovery in^c effluent	^{14}C recovery in^c CO$_2$ trap	^{14}C recovery in^c soil	total ^{14}C recovery^c
RT5L9	0.862	0.031	0.95	0.89	0.02	0.03	0.94
RT16L9	0.548	0.035	0.83	0.58	0.15	0.11	0.84
RT48L9	0.063	0.071	0.39	0.07	0.37	0.14	0.48
RT5L28	0.923	0.015	1.97	0.91	0.01	0.03	0.95
RT16L28	0.683	0.021	1.49	0.68	0.05	0.07	0.80
RT48L28	0.165	0.038	0.69	0.18	0.21	0.11	0.50
RT16L85	0.803	0.015	1.98	0.85	0.01	0.04	0.90
RT48L85	0.697	0.007	4.26	0.67	0.03	0.07	0.77

^{a} Steady-state relative 2,4-D concentration in column effluents. ^{b} First-order degradation rate constants and corresponding half-lives derived from C_s using eq 9. ^{c} As fractions of applied ^{14}C as [^{14}C]2,4-D.

The observed BTCs were then used to optimize first-order degradation rate constants (k_{1s}) as a function of different column conditions to separate effects of RT and v. Observed values of C_s were used to calculate (eq 9) column-specific k_{1s} values (Table 3), which were then used to predict 2,4-D BTCs (Figure 3). Results using this approach were similar to fitting the observed BTCs to the ADE including first-order degradation where the degradation rate constant ($k_{1\ LE}$ for LE model and $k_{1\ NE}$ for chemical NE model fits) was optimized. In fact, with the exception of one experiment (RT5L9), values of k_{1s} (using eq 9) were not significantly different from optimized $k_{1\ LE}$ values using the LE model (Table 4). Also, since it was shown that chemical NE may have been important in the sterile control column, observed BTCs were fit using the chemical NE model where β, ω, and $k_{1\ NE}$ were optimized (Table 4). Values of $k_{1\ NE}$ were again essentially identical to k_{1s} values obtained from eq 9 (or LE fitted $k_{1\ LE}$ values) for all conditions except those at a RT of 5.3 h. The variation of model estimates for degradation rate constants at the shortest column RT (5.3 h) can be partially explained by the fact that very little degradation occurred during transport in these columns (C_s values of 0.86 and 0.92), which results in extreme

sensitivity of the optimized rate constants to fluctuations in observed data about the steady-state position.

More importantly, our data show that column-derived k_{1s} values varied by approximately 1 order of magnitude (0.007−0.071 h^{-1}, Table 4) for the eight different column RT and v treatments. The variation in column-derived rate constants obtained in this study cannot be explained by variations in RT (Figure 4A) but does exhibit a dependence on pore water velocity. The relationship between optimized k_{1s} values and v showed that k_{1s} values remained relatively low at v above 1 cm h^{-1} but increased sharply at v below 1 cm h^{-1} (Figure 4B). To illustrate the observed relationship, a best-fit curve was included in Figure 4B of the form

$$k_{1s} = a + bv^{-1} \tag{10}$$

where a and b are fitted constants ($a = 0.014$ h^{-1}, $b = 0.011$ cm h^{-2}, $r^2 = 0.88$). The effects of v on column-derived rate constants observed in this study were in general agreement with results of Estrella et al. (8) and Kelsey and Alexander (9). First-order 2,4-D degradation rate constants obtained by

TABLE 4. Estimated First-Order Degradation Rate Constants and Nonequilibrium Parameters for Nonsterile Column Experiments Obtained Using Various Modeling Approaches (Values of R_f and D Obtained Independently)

experimental ID	k_{1s} from C_s[a] (h^{-1})	$k_{1\ LE}$ from LE model fit (h^{-1})	chemical NE model fit		
			$k_{1\ NE}$ (h^{-1})	β[b]	ω[c]
RT5L9	0.031	0.020	0.11	0.58	0.24
RT16L9	0.035	0.030	0.034	0.79	2.7×10^{-4}
RT48L9	0.071	0.069	0.070	0.77	1×10^{-7}
RT5L28	0.015	0.017	0.008	0.72	0.33
RT16L28	0.021	0.019	0.016	0.74	0.607
RT48L28	0.038	0.037	0.037	0.91	2.4×10^{-4}
RT16L85	0.015	0.012	0.014	0.82	4.7×10^{-4}
RT48L85	0.007	0.008	0.007	0.28	37.3

[a] Using eq 9. [b] $\beta = [1 + (\rho/\theta)FK_d]/R_f$, where F is the fraction of sorbent for which sorption is instantaneous. [c] $\omega = [k_2(1 - \beta)R_fL]/v$, where k_2 is the desorption rate constant.
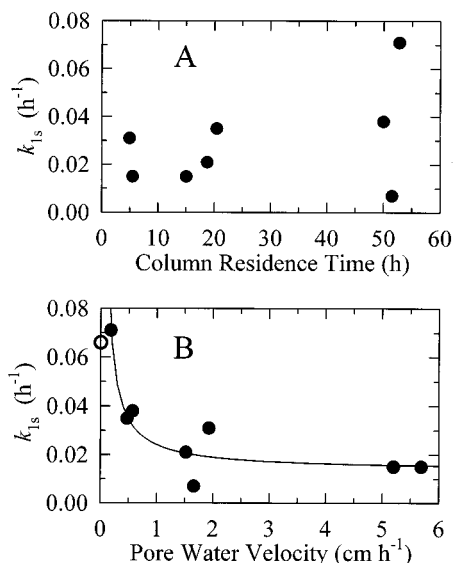

FIGURE 4. First-order degradation rate constants derived from [^{14}C]2,4-D steady-state effluent concentrations as a function of column residence time (A) and pore water velocity (B). The solid line in panel B represents the best-fit empirical function as described in the text, and the circle shown at $v = 0$ represents the degradation rate constant under batch conditions (k_{1b}).

FIGURE 5. First-order degradation rate constants derived from [^{14}C]2,4-D steady-state effluent concentrations as a function of column averaged local opportunity time, v^{-1}. The solid line represents the best-fit empirical function as described in the text.

Estrella et al. (8) increased from 0.04 h^{-1} at v of 4.7 h^{-1} (albeit from a saturated column experiment) to 0.14 h^{-1} at v of approximately 0.6 cm h^{-1} (unsaturated column). Likewise, higher v resulted in lower amounts of p-nitrophenol degradation during the early stages of column transport (9).

Discussion

Several factors may contribute to observed variations in apparent degradation rate constants as a function of pore water velocity. First, in a transport environment, it is not clear whether biomass concentrations responsible for 2,4-D degradation remain constant as a function of v (9). Higher v may result in greater microbial transport, hence reduce the accumulation of column biomass. A logistic growth model (coupled with the ADE) might successfully describe steady-state 2,4-D concentrations during transport if the population of 2,4-D degrading organisms were attenuated by an additional term describing the simultaneous decay of the population. Further, changes in v may change the microbial community structure, which could influence 2,4-D degradation rates. Given the difficulty in accurately enumerating members of the soil microbial community responsible for 2,4-D degradation, further work using molecular techniques would be necessary to determine the sensitivity of the microbial community to changes in pore water velocity.
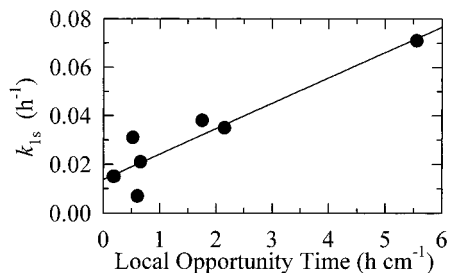
Second, increases in v may result in lower concentrations of inorganic nutrients or organic substrates important for cometabolism of 2,4-D. The slow desorption of constituents required for optimal microbial growth and 2,4-D degradation may be compounded when v exceeds characteristic desorption rates. In the current study, 3 mM CaCl$_2$ was used as a background solution, and it is uncertain whether nutrient availability affected rates of 2,4-D degradation.

Third, apparent degradation rate constants may decrease with increasing v due to decreases in residence time per unit length (or per unit area or volume). The residence time per unit length may be thought of as a *local opportunity time*. At sufficiently high v, apparent degradation rate constants may decline because advective velocity exceeds characteristic times required for the sequence of elementary reactions describing microbial degradation (e.g., membrane transport, enzymatic reactions). Our data support such a relationship between the column-derived first-order rate constants and the column-averaged local opportunity times (Figure 5). One might hypothesize that at infinitely large local opportunity times (i.e., $v \rightarrow 0$), apparent rate constants would approach those determined under batch conditions. Interestingly, the higher rate constants determined at large local opportunity times (low v) did approach the batch-determined rate constant of $\sim$0.07 h^{-1} (Figure 4B).

Differences in apparent degradation rate constants under batch vs column conditions with varying v are further complicated by the effects of v on mass transfer rates. Under batch conditions, it has been shown that degradation rate constants may be constrained by mass transfer rates of 2,4-D (i.e., desorption limited degradation) to sites of microbial degradation (28, 29). Several studies (20, 30–32) have shown that increases in v result in greater estimates of column-derived mass-transfer rate parameters affecting sorbing solutes (e.g., values of ω in the chemical NE model). Consequently, when degradation rates are desorption-limited (30), increases in v may increase degradation rates during transport. However, data obtained in this study on the

relationship between ν and apparent degradation rate constants do not support this hypothesis.

In summary, the effects of pore water velocity on microbial degradation rates may be confounded by several processes operating simultaneously: (i) effects of ν on density and/or distribution of microbial biomass responsible for degradation, (ii) effects of ν on nutrient concentrations in the soil solution which may affect microbial degradation rates, (iii) effects of ν on local opportunity times that may be required for maximum degradation rates, and (iv) effects of ν on solute mass transfer rates. The relative contribution of each of these processes in controlling contaminant degradation rates during transport will require further experimentation. However, results from the current study demonstrate that ν (independent of residence time) has a significant effect on 2,4-D degradation rate constants. This finding emphasizes the difficulty in accurately predicting the degradation and transport of organic contaminants in soils across a range of flow conditions using independently determined rate parameters.

Acknowledgments

Literature Cited

(1) Boesten, J. J. T. I.; van der Linden, A. M. A. *J. Environ. Qual.* **1991**, *20*, 425−435.

(2) Villeneuve, J.-P.; LaFrance, P.; Banton, O.; Frechette, P.; Robert, C. *J. Contam. Hydrol.* **1988**, *3*, 77−96.

(3) Carsel, R. F.; Smith, C. N.; Mulkey, L. A.; Dean, J. D.; Jowise, P. *User manual for the Pesticide Root Zone Model (PRZM)*, Release 1. U.S. EPA: Washington, DC, 1984; Report 60013-84-109.

(4) Nofziger, D. L.; Hornsby, A. G. *Chemical Movement in Layered Soils: User's Manual;* Florida Cooperative Extension Service, Institute of Food and Agriculture Science, University of Florida: Gainesville, FL, 1987; Cir. 780.

(5) Wagenet, R. J.; Hutson, J. L. *LEACHM: Leaching estimation and chemistry model. A process based model for water and solute movement, transformations, plant uptake and chemical reactions in the unsaturated zone. Continuum Vol. 2*; Water Resource Institute, Cornell University: Ithaca, NY, 1989.

(6) Toride, N.; Leij, F. J.; van Genuchten, M. T. *The CXTFIT code for estimating transport parameters from laboratory or field tracer experiments, Version 2.0*; Research Report 137; U.S. Salinity Laboratory, ARS, USDA: Riverside, CA, 1995.

(7) Angley, J. T.; Brusseau, M. L.; Miller, W. L.; Delfino, J. J. *Environ. Sci. Technol.* **1992**, *26*, 1404−1410.

(8) Estrella, M. R.; Brusseau, M. L.; Maier, R. S.; Pepper, I. L.; Wierenga, P. J.; Miller, R. M. *Appl. Environ. Microbiol.* **1993**, *59*, 4266−4273.

(9) Kelsey, J. W.; Alexander, M. *Soil Sci. Soc. Am. J.* **1995**, *59*, 113−117.

(10) Pivetz, B. E.; Steenhuis, T. S. *J. Environ. Qual.* **1995**, *24*, 564−570.

(11) Baskaran, S.; Bolan, N. S.; Rahman, A.; Tillman, R. W. *Pestic. Sci.* **1996**, *46*, 333−343.

(12) van Genuchten, M. Th.; Wierenga, P. J. Solute dispersion coefficients and retardation factors. In *Methods of soil analysis, Part I*; Klute, A., Ed.; American Society of Agronomy: Madison, WI, 1986; Vol. 9, pp 1025−1054.

(13) Wolf, D. C.; Dao, T. H.; Lavy, T. L. *J. Environ. Qual.* **1989**, *18*, 39−44.

(14) Monod, J. *Annu. Rev. Microbiol.* **1949**, *3*, 371−394.

(15) Simkins, S.; Alexander, M. *Appl. Environ. Microbiol.* **1984**, *47*, 1299−1306.

(16) Characklis, W. G. Kinetics of microbial transformations. In *Biofilms*; Characklis, W. G., Marshall, K. C., Eds.; Wiley: New York, 1990; p 233.

(17) Ogram, A. V.; Jessup, R. E.; Ou, L. T.; Rao, P. S. C. *Appl. Environ. Microbiol.* **1985**, *49*, 582−587.

(18) Brusseau, M. L.; Rao, P. S. C. *Crit. Rev. Environ. Control* **1989**, *19*, 33−99.

(19) Brusseau, M. L.; Jessup, R. E.; Rao, P. S. C. *Water Resour. Res.* **1989**, *25*, 1971−1988.

(20) Gaber, H. M.; Inskeep, W. P.; Comfort, S. D.; Wraith, J. M. *Soil Sci. Soc. Am. J.* **1995**, *59*, 60−67.

(21) van Genuchten, M. T.; Wagenet, R. J. *Soil Sci. Soc. Am. J.* **1989**, *53*, 1301−1310.

(22) van Genuchten, M. T.; Parker, J. C. *Soil Sci. Soc. Am. J.* **1984**, *48*, 703−708.

(23) van Genuchten, M. T.; Alves, W. J. *Analytical Solutions of the one-dimensional convective-dispersive solute transport equation*; Technical Bulletin 1661; U.S. Department of Agriculture: Washington, DC, 1982.

(24) Alexander, M.; Scow, K. M. Kinetics of biodegradation in soil. In *Reactions and movement of organic chemicals in soils*; Sawhney, B. L., Brown, K. Eds.; Soil Science Society of America: Madison, WI, 1989; pp 243−269.

(25) Parker, L. W.; Doxtaedar, K. G. *J. Environ. Qual.* **1982**, *11*, 679−684.

(26) Valocchi, A. J. *Water Resour. Res.* **1985**, *21*, 808−820.

(27) Bahr, J. M.; Rubin, J. *Water Resour. Res.* **1987**, *23*, 438−452.

(28) Scow, K. M.; Alexander, M. *Soil Sci. Soc. Am. J.* **1992**, *56*, 128−134.

(29) Chung, G.-Y.; McCoy, B. J.; Scow, K. M. *Biotechnol. Bioeng.* **1993**, *41*, 625−632.

(30) Gamerdinger, A. P.; Lemley, A. T.; Wagenet, R. J. *J. Environ. Qual.* **1991**, *20*, 815−822.

(31) Brusseau, M. L. *J. Contam. Hydrol.* **1992**, *9*, 353−368.

(32) Darland, J. E.; Inskeep, W. P. *Environ. Sci. Technol.* **1997**, *31*, 704−709.

(33) Pignatello, J. J.; Xing, B. *Environ. Sci. Technol.* **1996**, *30*, 1−11.